Paramagnetic resonance spectrum of metastable ^2P atomic nitrogen

Gerald J. Diebold
Brown University, Department of Chemistry, Providence, Rhode Island 02912

David L. McFadden
Boston College, Department of Chemistry, Chestnut Hill, Massachusetts 02167
(Received 30 June 1981)

The paramagnetic resonance spectrum of metastable $^2P_{3/2}$ atomic nitrogen has been observed downstream from an electrodeless discharge in nitrogen-helium gas mixtures. The g factors for the nine observed transitions deviate significantly from the Lande formula. Analysis of the Zeeman effect shows that the departure from Lande formula is caused by an intermediate Paschen-Back effect which occurs in magnetic fields of only a few kilogauss. The nuclear hyperfine structure has been analyzed (for the ^{14}N nucleus) and coupling parameters determined. The fine-structure interval for the ^2P states has been measured to be $12\,970 \pm 80$ MHz.

I. INTRODUCTION

The importance of nitrogen in astronomy and atmospheric science as well as in the laboratory has motivated detailed investigations of this atom throughout the history of spectroscopy. Recently, there has been additional interest in the high-resolution spectrum of nitrogen since nuclear hyperfine splittings of energy levels provide a sensitive test for *ab initio* calculations of electronic wave functions. In nitrogen the $1s^2 2s^2 2p^3$ configuration gives rise to three terms, ^4S, ^2D, and ^2P, between which electric dipole transitions are forbidden by the Laporte rule, so that the ^2D and ^2P states are metastable.

The paramagnetic resonance spectrum of the ^4S ground state has been analyzed by Heald and Beringer[1] and at a later date by Zak and Shugart.[2] Evenson and Radford[3] recorded the ^2D spectrum with an EPR spectrometer used in conjunction with a discharge-flow system, and have determined the fine-structure splitting within the D doublet as well as the nuclear hyperfine coupling parameters.[4] Less precise determinations of the fine-structure interval for the ^2P states have been reported by McConkey,[5] and Kaufman and Ward[6] using optical spectroscopy. *Ab initio* calculations of wave functions and hyperfine coupling parameters appear in papers by Clementi, Roothaan, and Yoshimine,[7] Schaefer and co-workers,[8–10] and Beltran-Lopez and Gonzalez E.[11]

This paper presents an analysis of the electron paramagnetic resonance (EPR) spectrum of the $^2P_{3/2}$ state of ^{14}N. The small fine-structure splitting within the P doublet causes an intermediate Paschen-Back effect at the magnetic fields employed in these experiments. Thus, both the intensities of the transitions and the observed g factors deviate significantly from their values as given by pure Russell-Saunders coupling. The fine-structure splitting and the nuclear-hyperfine-coupling parameters were determined by a least-squares fit to the experimental data where the energy level of each M state was determined by direct diagonalization of the perturbation matrix of the spin orbit, Zeeman, and magnetic-dipole hyperfine operators.

II. EXPERIMENTAL

The ^2P states were produced as described in Ref. 12. Briefly, a 1% mixture of nitrogen in helium was passed through an electrodeless microwave discharge (2450 MHz) located several centimeters upstream of the EPR cavity. A small amount of SF_6 was introduced into the gas flow downstream from the discharge to reduce electron-generated noise in the spectrometer as described in Refs. 12 and 13. The metastable ^2P states were then detected in a conventional field modulation EPR spectrometer where the klystron frequency is locked to a cavity resonance, and the Zeeman field varied.

Magnetic resonance is detected at the field modulation frequency (100 kHz) with a lock-in amplifier and the first derivative of the absorption profile displayed. The $^2P_{3/2}$ spectrum is presented in Fig. 1. The largest splittings that divide the spectrum into three groups of lines are due to mixing of the $J=\frac{3}{2}$ and $\frac{1}{2}$ states by the magnetic field (intermediate Paschen-Back effect). The splittings within each group are caused by the magnetic-dipole-hyperfine-structure interaction that arises from the unit nuclear spin of the ^{14}N isotope. The increasing baseline in the figure is the result of free electrons interacting with the microwave fields. In order to optimize the signal intensity, the gas velocity was increased until the electron noise was on the threshold of interfering with the operation of the spectrometer.

Magnetic fields were determined by calibrating the Hall probe in the spectrometer against a nuclear-magnetic-resonance (NMR) field probe. The NMR probe was too large to fit inside the EPR cavity and thus it was necessary to remove the cavity and flow tube for the calibration. No correction was made for the difference in magnetic field at the center of the magnet gap with the cavity in place. The klystron frequency was determined by recording the field where the atomic oxygen $^3P_{2,1}$ transition appeared, which with the known g factor was used to calculate a value for the klystron frequency. The apparatus required to measure the klystron frequency directly during the recording of each EPR line was not available for these experiments.

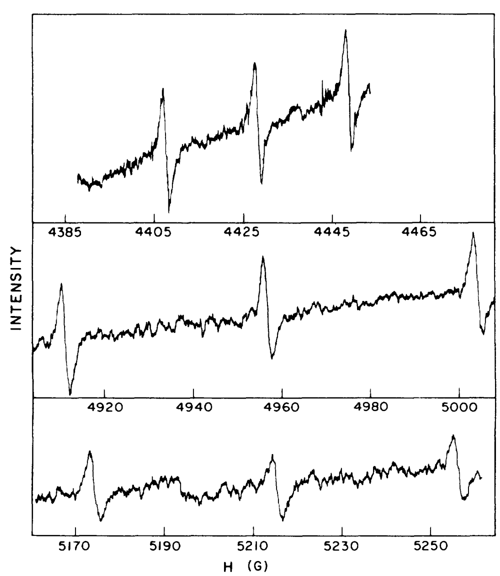

FIG. 1. EPR spectrum of $^2P_{3/2}$ nitrogen.

III. ANALYSIS

If the influence of the nuclear moment is neglected, the coupling of angular momenta in ^2P atomic nitrogen can be described at low magnetic fields by a Russell-Saunders basis set $|LSJM\rangle$, where the orbital angular momentum $\vec{L}$ and the spin angular momentum $\vec{S}$ couple to form a resultant total angular momentum $\vec{J}$, with a fixed component M along the field direction. In the limit of high magnetic field (the Paschen-Back limit) $\vec{L}$ and $\vec{S}$ uncouple and precess individually about the direction of the external magnetic field (with components M_L and M_S in the direction of the field) and the wave functions are most conveniently expressed in an $|LM_LSM_S\rangle$ basis. Between these extreme cases, the coupling is intermediate and the wave functions become linear combinations of either set of basis functions. Analytic expressions for the wave functions for any L doublet are given in Ref. 4, and expressions for the energy levels of any M state as a function of magnetic field are given in Refs. 4 and 14. By subtraction of the energy-level formulas, expressions are obtained that can be solved for the field at which allowed magnetic-dipole transitions ($\Delta M=\pm 1$) are observed for a given fine-structure splitting and klystron frequency. Figure 2 is a plot of the fields at which the allowed transitions within a P doublet take place as the fine-structure splitting δ is varied. The transitions in Fig. 2 correspond to those marked in the energy-level diagrams given in Fig. 3, which were calculated by evaluating expressions for the energy of any M state as a function of the magnetic field parameter $x=(g_s-g_l)\,\mu_B H/\delta$, where g_s and g_l are the electronic g factors for spin and orbital angular momentum respectively, μ_B is the Bohr magneton, and H is the magnitude of the magnetic field.

As expected, Fig. 2 shows that for large values of the fine-structure interval compared with the perturbing field (i.e., $x<<1$) the g factors correspond to their values in pure Russell-Saunders coupling, $\frac{4}{3}$ and $\frac{2}{3}$. On the other hand, when the fine-structure interval becomes small the field parameter for a given transition may be much greater than one indicating a complete Paschen-Back effect so that the g factors approach values of 1 or 2. Note in Fig. 2 that the g factors for

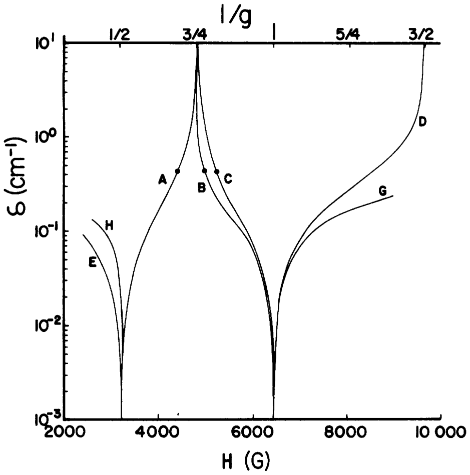

FIG. 2. Magnetic fields, or equivalently, g factors for ^2P transitions as a function of the magnitude of the fine-structure interval δ, calculated by equating the klystron frequency (9 GHz) to the frequency corresponding to a given pair of field-dependent energy levels and solving the resulting nonlinear equation using Newton's method. Letters correspond to transitions marked in Fig. 3. The abscissa is linear in the magnetic field or, equivalently, the inverse of the g factor. Note that transition F does not fall within the plotted range of the field. Dots indicate the field positions of the observed lines.

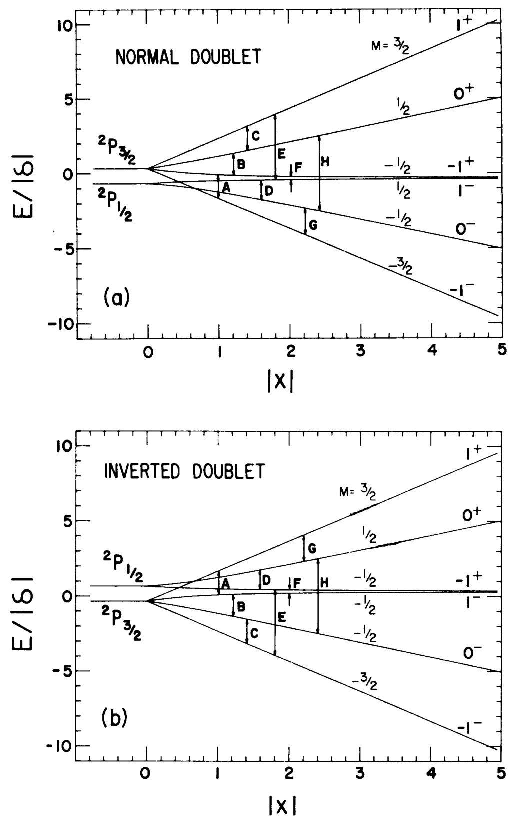

FIG. 3. Energy levels of (a) normal and (b) inverted P doublets as a function of the magnitude of the field parameter $x=(g_s-g_l)\mu_B H/\delta$, as calculated from Eq. (2) in Ref. 3. The notation (in the high field limit) refers to values of M_L with a superscript of M_S denoting wave functions of the form $|1M_L\,\frac{1}{2}M_S\rangle$.

transitions E, H, and G have values of 2 and 1 in the Paschen-Back limit where spin-orbit coupling acts only to perturb the Paschen-Back wave functions; as x becomes small compared with one, a g factor is not normally defined for these transitions. Note also that a transition between a given pair of states may take place at different fields depending upon whether the doublet is normal or inverted. The $(^2P_{3/2})\frac{3}{2}\leftarrow\frac{1}{2}$ transition in a normal doublet, for instance, takes place at fields described by curve C in Fig. 2, whereas the same transition in an inverted doublet follows curve G. A measurement of the field positions of the $^2P_{3/2}$ transitions in the intermediate coupling case by itself does not permit a determination of whether the doublet is normal or inverted. From Figs. 1 and 2, it is evident that the experimentally observed spectrum can be assigned to transitions A, B, and C. The three dots in Fig. 2 are placed to correspond to the fine-structure splitting for the ^2P term, 0.4 cm^{-1}.

The origin of the intensity pattern of the transitions in the experimental spectrum is not intuitively obvious and deserves some comment. The intensity of any transition depends upon the transition line strength and the population difference between the initial and final states. The line strength can be determined by evaluation of matrix elements[15] of the operator

$$\vec{\mu}\cdot\vec{\mathrm{H}}_1=\sum_q(-1)^q\mu_q H_{-q}\ , \tag{1}$$

where the magnetic-dipole operator $\vec{\mu}$, defined by $\vec{\mu}=\mu_B(g_l\vec{\mathrm{L}}+g_s\vec{\mathrm{S}})$, and $\vec{\mathrm{H}}_1$, the microwave magnetic field, have been expressed (in standard tensor notation[16]) in terms of irreducible tensor operators for facile evaluation of matrix elements. In the case of pure Russell-Saunders coupling and where the nuclear moment is coupled to the external Zeeman field (i.e., uncoupled from the electronic field at the nucleus), the line strengths for a given J and M are given by

$$|\langle JM+1|\mu_{+1}|JM\rangle|^2=\tfrac{1}{2}g^2(J-M)(J+M+1)\ , \tag{2}$$

where g is the Lande g factor and M refers to the lower state in the transition. In a basis set $|LSJMIM_I\rangle$ the nuclear spin I has no influence on the intensity pattern other than to decrease the population difference between a pair of levels through splitting of the energy levels. The selection rule $\Delta M_I=0$ follows since $\vec{\mu}$ does not operate on the nuclear-spin wave function.

The effect of intermediate coupling is to mix wave functions with the same values of M by an amount dependent on the field parameter; matrix elements of the operator in Eq. (1) must therefore be computed with field-dependent wave functions in order to determine the transition strength at any field. Radford and Evenson[4] have given analytic expressions for the coupling coefficients using Russell-Saunders basis functions so that the field-dependent wave function $|JMx\rangle$ can be written in terms of field-dependent coupling coefficients $C_1(x)$ and $C_2(x)$, and field-independent wave functions $|JM\rangle$ (where the L and S quantum numbers have been deleted). The transition $(^2P_{3/2})\ \frac{3}{2}\leftarrow\frac{1}{2}$, for instance, has a line strength given by

$$|\langle\tfrac{3}{2}\tfrac{3}{2}x\,|\mu_{+1}|\,\tfrac{3}{2}\tfrac{1}{2}x\rangle|^2 = |C_1(x)\langle\tfrac{3}{2}\tfrac{3}{2}\,|\mu_{+1}|\,\tfrac{1}{2}\tfrac{1}{2}\rangle + C_2(x)\langle\tfrac{3}{2}\tfrac{3}{2}\,|\mu_{+1}|\,\tfrac{3}{2}\tfrac{1}{2}\rangle|^2\,, \quad (3)$$

where $C_1(x)$ and $C_2(x)$ are as given in Ref. 4 and the field-independent matrix elements $[-(\frac{1}{3})^{1/2}$ and $-(\frac{8}{3})^{1/2}$, respectively] are calculated by standard tensor operator methods.[15] Figure 4 gives

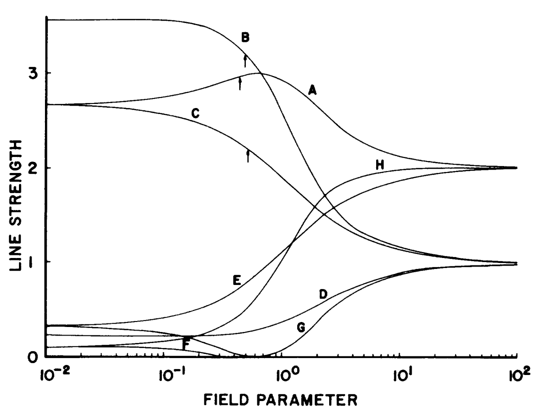

FIG. 4. Field-dependent line strengths (in arbitrary units) for ^2P transitions A through F marked in Fig. 3 as a function of the magnitude of the field parameter x calculated from matrix elements of μ_{+1} with field-dependent wave functions. The arrows mark the positions of the experimentally determined transitions.

line strengths as a function of the field parameter for transitions marked in Fig. 3. At low values of the magnitude of the field parameter the relative intensities for transitions A through D are $\frac{2}{9}$: $\frac{24}{9}$: $\frac{32}{9}$: $\frac{24}{9}$ as given by Eq. (2) above. As the Paschen-Back limit is approached these transition strengths approach values of 2 or 0, as can be verified by direct calculation of matrix elements of μ_{+1} with Paschen-Back wave functions, or by calculating limiting values of $C_1(x)$ and $C_2(x)$ and substitution in expressions such as Eq. (3). Note that the coupling coefficients are not even functions of x. This means that, in general, line strengths for two given states are different for normal and inverted terms. The $(^2P_{3/2})-\frac{1}{2}\leftarrow-\frac{3}{2}$ transition, for example, has a field-dependent transition strength governed by curve A in the case of a normal doublet, whereas the same transition corresponds to curve C when the levels are inverted. Of course, when the field parameter approaches zero, the two curves have the same line strength, as Fig. 4 shows. The agreement between the experimental intensities and the curves in Fig. 4 is good given the moderately high background noise in the spectrometer. Note that in several recordings of the spectrum, the high field group of lines was always of low intensity—the other two groups varied in relative intensity. The relatively small line strength for the $(^2P_{1/2})\ \frac{1}{2}\leftarrow-\frac{1}{2}$ transition accounts for our failure to observe this line experimentally.

IV. HYPERFINE STRUCTURE

The intermediate coupling of the angular momenta in ^2P nitrogen at moderate fields means that a calculation of hyperfine splittings must be carried out using field-dependent wave functions, or by direct diagonalization of the perturbation Hamiltonian. The latter approach has been chosen here.

Since the p^3 configuration of nitrogen is a half-filled shell, the conventional spin-orbit interaction does not contribute to the fine-structure splitting in first order. The interaction of the spin of one electron with the orbit of the other electrons and the spin-spin interaction give rise to the fine-structure splittings within the ^2D and ^2P states, and at the same time mix the wave functions of the ^4S, ^2D, and ^2P states.[17] It is the spin-spin interaction that is primarily responsible for the fine-structure splittings within the ^2D and ^2P states whereas the spin-other-orbit interaction acts to mix the zero-field Russell-Saunders basis functions thereby altering the g factors of all three states. A first-order perturbation calculation shows that changes in the g factors of the ^2P states are given by[18,11]

$$\Delta g(^2P_{1/2})=0\ ,$$
$$\Delta g(^2P_{3/2})=\frac{2}{3}\left[\frac{\zeta'^2}{(E_P-E_S)^2}-\frac{\zeta'^2}{(E_P-E_D)^2}\right],\tag{4}$$

where ζ' is the spin-orbit parameter, and E_P, E_D, and E_S are the term energies of the unperturbed Russell-Saunders states. A value[19] for ζ' has been estimated to be 69 cm^{-1} thus giving a change in the g factor of the $^2P_{3/2}$ levels of -3×10^{-5}. Note that the magnetic field does not act to change the relative amount of jj-coupling in the p^3 configuration. Since the deviation of the angular momentum coupling from the pure Russell-Saunders coupling scheme has a negligible effect on the g factors, all matrix elements were calculated within the P doublet in an unperturbed $|LSJMIM_I\rangle$ basis. The small departure of the ^2P states from Russell-Saunders coupling further means that the spin-orbit operator (normally a sum over scalar products of the orbital and spin angular momenta of the three p electrons) simplifies to a single term[14] proportional to $\vec{\mathrm{L}}\cdot\vec{\mathrm{S}}$.

In this approximation, the Zeeman and spin-orbit operator is given by

$$\mathscr{H}_1=\zeta\vec{\mathrm{L}}\cdot\vec{\mathrm{S}}+\mu_B(g_l\vec{\mathrm{L}}+g_s\vec{\mathrm{S}}-g_I\vec{\mathrm{I}})\cdot\vec{\mathrm{H}}\ ,\tag{5}$$

where ζ, the spin-orbit coupling parameter, is related to the fine-structure interval through $\delta=\zeta(L+\frac{1}{2})$. The diagonal elements of the Zeeman operator for an L doublet are given by

$$\langle L\,\tfrac{1}{2}\,JMIM_I\,|\,\mathscr{H}_1\,|\,L\,\tfrac{1}{2}\,JMIM_I\rangle=\frac{\zeta}{2}[J(J+1)-L(L+1)-\tfrac{3}{4}]$$
$$+\frac{[J(J+1)-L(L+1)+3/4]}{2J(J+1)}\mu_B(g_s-g_l)HM+\mu_B g_l HM-g_I HM_I\ .\tag{6}$$

Off-diagonal elements, which give rise to the Paschen-Back effect, are given by

$$\langle L\tfrac{1}{2}L+\tfrac{1}{2}MIM_I\,|\,\mathscr{H}_1\,|\,L\tfrac{1}{2}L-\tfrac{1}{2}MIM_I\rangle=-\frac{\mu_B(g_s-g_l)H}{2}\left[1-\left[\frac{2M}{2L+1}\right]^2\right]^{1/2}.\tag{7}$$

The magnetic-dipole hyperfine interaction can be described by the operator[20,21]

$$\mathscr{H}_2=2g_I\mu_B^2\Big[\langle r_l^{-3}\rangle\vec{\mathrm{L}}\cdot\vec{\mathrm{I}}+\xi\langle r_s^{-3}\rangle[L(L+1)(\vec{\mathrm{S}}\cdot\vec{\mathrm{I}})-\tfrac{3}{2}(\vec{\mathrm{L}}\cdot\vec{\mathrm{S}})(\vec{\mathrm{L}}\cdot\vec{\mathrm{I}})$$
$$-\tfrac{3}{2}(\vec{\mathrm{L}}\cdot\vec{\mathrm{I}})(\vec{\mathrm{L}}\cdot\vec{\mathrm{S}})]+\frac{8\pi}{3}\,|\,\psi(0)\,|^2(\vec{\mathrm{S}}\cdot\vec{\mathrm{I}})\Big]\ ,\tag{8}$$

where ξ is given by[22]

$$\xi=\frac{(2l+1)-4S}{S(2l-1)(2l+3)(2L-1)}\ .$$

This operator allows for the possibility that the radial integral of the electronic charge density and spin density can differ. The effect of this, when the contact term $|\psi(0)|^2$ is included, is that there are three adjustable parameters that can be varied to fit an experimentally observed spectrum. Matrix elements of this operator for $S=\frac{1}{2}$ are given by

$$\langle L\,\tfrac{1}{2}\,JMIM_I\,|\,\mathscr{H}_2\,|\,L\,\tfrac{1}{2}\,JM'IM_I'\rangle$$
$$=ha_J\sum_q(-1)^{q+J-M+I-M_I}[J(J+1)(2J+1)I(I+1)(2I+1)]^{1/2}\begin{bmatrix}J&1&J\\-M&q&M'\end{bmatrix}\begin{bmatrix}I&1&I\\-M_I&-q&M_I'\end{bmatrix},\tag{9}$$

where

$$ha_J = 2g_I\mu_B^2\left[\langle r_l^{-3}\rangle \frac{[J(J+1)+L(L+1)-3/4]}{2J(J+1)} + \langle r_s^{-3}\rangle\xi\left[\frac{L(L+1)[J(J+1)-L(L+1)+3/4]}{2J(J+1)} - \frac{3}{4}\frac{[J(J+1)-3/4]^2-[L(L+1)]^2}{J(J+1)}\right] + \frac{8\pi}{6}|\psi(0)|^2\frac{[J(J+1)-L(L+1)+3/4]}{J(J+1)}\right],$$

and

$$\langle L\tfrac{1}{2}L+\tfrac{1}{2}MIM_I|\mathscr{H}_2|L\tfrac{1}{2}L-\tfrac{1}{2}M'IM_I'\rangle = ha_{J,J-1}\sum_q(-1)^{q+J-M+I-M_I}[L(2L+1)(2L+2)I(I+1)(2I+1)]^{1/2} \times \begin{pmatrix} L+\frac{1}{2} & 1 & L-\frac{1}{2} \\ -M & q & M' \end{pmatrix}\begin{pmatrix} I & 1 & I \\ -M_I & -q & M_I' \end{pmatrix}, \quad (10)$$

where

$$ha_{J,J-1} = 2g_I\mu_B^2\left[\frac{\langle r_l^{-3}\rangle}{2L+1} + \langle r_s^{-3}\rangle\xi\left[\frac{3/4}{2L+1} - \frac{L(L+1)}{2L+1}\right] - \frac{8\pi}{3}\frac{|\psi(0)|^2}{2L+1}\right].$$

In expressions (9) and (10), q is summed over the values 1, 0, and -1; however, for given values of M and M', q is restricted to a single value since the sum of the bottom-row elements of the first 3-j symbol in each sum must be zero. Thus, only one value of q occurs in the summation for a given M and M', which in turn fixes the difference between M_I and M_I'.

The ^2P states can show an electrostatic quadrupole interaction with the nucleus as a result of polarization of the valence electrons. The electric quadrupole Hamiltonian has been given in Ref. 21 [Eq. (65)], matrix elements of which are given in Ref. 4 [Eq. (11)]. In the analysis of the ^2P spectrum, the first-order quadrupole interaction contributes diagonal terms to the Hamiltonian matrix with a single adjustable parameter, $b_{3/2}$.

The perturbation Hamiltonian for the $|1\frac{1}{2}JMIM_I\rangle$ states gives an 18×18 symmetric matrix. Marquardt's method,[23] was used to find least-squares values for the five adjustable parameters. This procedure is a straightforward, iterative numerical technique; the computation of the derivative of the calculated line position with respect to the adjustable parameter deserves some comment, however, since numerical differentiation of eigenvalues was found to be unsatisfactory. Consider a Hamiltonian $\mathscr{H}$, which is diagonalized by the transformation $E = U^\dagger\mathscr{H}U$, where U and its Hermitian complex $U^\dagger$ are matrices, and E is a vector of eigenvalues. If each of these quantities is expanded in a Taylor series, the first-order correction to the eigenvalue vector ΔE for a change $\Delta\mathscr{H}$ in the Hamiltonian is given by $\Delta E = U^\dagger(\Delta\mathscr{H})U$. Thus, in the numerical calculation, U is found for given values of the variable parameters and the magnetic field, and the change in the eigenvalue vector is calculated for changes in one of the variable parameters. The derivative of the line position with respect to a change in any parameter is found by subtracting the appropriate members of the eigenvalue vector. The numerical calculation converged after only a few iterations, and gave the parameters listed in Table I, where the errors were determined by the least-squares procedure. The experimental data were fit to within an average of 7 MHz. This relatively large error is a consequence of a somewhat less than ideal calibration method for both the field positions of the lines and the klystron frequency.

V. DISCUSSION

In principle, EPR spectrometry provides a method for determining whether an electronic term is normal or inverted by comparison of the experi-

TABLE I. $^{14}N\,^2P$ fine-structure interval and hyperfine coupling parameters. The results from Ref. 4 are based on ^2D experimental data; those from Ref. 8 are theoretical values calculated with polarization wave functions.

	This work	Reference 4	Reference 8
δ	-12970 ± 80 MHz $(-0.4326\pm0.003\ \mathrm{cm}^{-1})$		
$a_{3/2}$	63.0 ± 5	63.4 MHz	62.6 MHz
$a_{1/2}$	306 ± 100	319.3	314.3
$a_{3/2,1/2}$	16.9 ± 9	17.6	
$b_{3/2}$	-0.3 ± 7		0.05

mental signal intensities with the calculated line strengths. If thermal equilibrium is maintained for states within a term, relative ordering of the energies of each J state can be carried out based on the population dependence of the line intensity. Unfortunately, this method is not sensitive unless the fine-structure interval is at least comparable to kT (where k is Boltzmann constant and T is the temperature of the gas). Thus, with the experimental data given here it is not possible to determine the relative energies of the $^2P_{3/2}$ and $^2P_{1/2}$ states. The fine-structure interval reported here[24] is in excellent agreement with the previously measured values given in Refs. 5 and 6 where intrinsically lower resolution techniques were employed.

The agreement between the experimental results from this work and the predicted hyperfine coupling parameters given by Radford and Evenson[4] is well within the experimental error. The coupling parameters calculated by Radford and Evenson for the ^2P states are based on an assumption of transferability of the values of the radial integrals within the p^3 configuration. (This was done to give an accurate test of the validity of the three-parameter theory of hyperfine coupling.) Based on *ab initio* calculations of the radial integrals, Schaefer and Klemm[8] have shown that this supposition is, in general, not valid. In atomic nitrogen, for instance, the contact term in the p^3 configuration shows significant variation among the ^4S, ^2D, and ^2P terms for calculations based on either polarization or first-order wave functions.[8] On the other hand, the same calculations show that the values of $\langle r_l^{-3}\rangle$ and $\langle r_s^{-3}\rangle$ vary by only a few percent between these states; thus, since the contact term makes only a small contribution to the hyperfine coupling parameters the above assumption made by Radford and Evenson appears valid for the three lowest terms of nitrogen.

The contributions of polarization, correlation, and relativistic effects are accounted for in the three-parameter hyperfine operator, Eq. (8). A detailed discussion of the three-parameter formulation of hyperfine interactions as well as the significance of these effects can be found in Ref. 25. A measure of the importance of the above effects is indicated by the departure of the quantity

$$\Delta=(\langle r_s^{-3}\rangle/\langle r_l^{-3}\rangle)-g_s/2$$

from zero.[26] For the doublet P states the radial integrals can be calculated by inverting Eqs. (9) and (10), which give

$$\begin{bmatrix} \langle r_l^{-3}\rangle \\ \langle r_s^{-3}\rangle \\ \frac{8\pi}{3}\,|\psi(0)|^2 \end{bmatrix} = \frac{h}{2g_I\mu_B^2}\begin{bmatrix} \frac{5}{6} & \frac{1}{6} & \frac{2}{3} \\ -\frac{5}{9} & \frac{5}{9} & \frac{10}{9} \\ \frac{10}{9} & -\frac{1}{9} & -\frac{16}{9} \end{bmatrix}\begin{bmatrix} a_{3/2} \\ a_{1/2} \\ a_{3/2,1/2} \end{bmatrix}.$$

The integrals (calculated with $\mu=0.4036$ nuclear magnetons) are

$$\langle r_l^{-3}\rangle=(20.1\pm4)\times10^{24}\ \mathrm{cm}^{-3},$$

$$\langle r_s^{-3}\rangle=(26.9\pm10)\times10^{24}\ \mathrm{cm}^{-3},$$

and

$$\frac{8\pi}{3}\,|\psi(0)|^2=(1.04\pm4)\times10^{24}\ \mathrm{cm}^{-3},$$

where the errors were calculated as in Ref. 23. The parameter Δ is thus 0.339 ± 0.2, indicating a relatively large departure of the hyperfine coupling from the predictions of the two-parameter theory. The results agree with the calculations of Schaefer and Klemm[8] which are within experimental uncertainties reported here; unfortunately, the inaccuracy of the experimental data precludes any comparison with the detailed calculations given in Ref. 11 for the p^3 states of nitrogen.

Since the uncertainties reported here are relatively large, some comment is in order. The source of the error is attributable to inaccurate determination of both the magnetic field within the flow tube and the klystron frequency. Unfortunately, the apparatus for accurate measurement of these was not available for this work. It is clear from the results of the least-squares procedure, however, that the errors are predominantly systematic; that is, the deviation of all the lines from the least-squares fit by approximately the same amount indicates some systematic error in the experimentally determined fields or klystron frequency. Although the data could be arbitrarily corrected to give an artificial improvement in the fit, no method for determining the magnitude of these errors is evident and therefore the data have been analyzed without correction. In fact, the errors in some of the parameters should be smaller than the limits given above since a small uniform displacement of all the lines, for example, does not simulate a change in the nuclear quadrupole coupling constant. (Additional figures have been included in the reported values of the hyperfine coupling constants and radial integrals to reflect the possible higher accuracy than is indicated by the least-squares procedure.) Even with the inaccuracy of the measurements an improved value for the fine-structure interval and a reasonably accurate value of $a_{3/2}$ have been determined. The value of $a_{3/2,1/2}$ can be expected to be less precisely determined than the other two hyperfine coupling parameters since it appears off the diagonal. A determination of $a_{1/2}$ is made possible only in that the $^2P_{1/2}$ states are mixed with the $^2P_{3/2}$ states.

Support of this research by the Petroleum Research Fund administered by the American Chemical Society, the Research Corporation, and the Office of Naval Research (Power Program) is gratefully acknowledged.

[1]M. A. Heald and R. Beringer, Phys. Rev. 96, 645 (1954).

[2]B. D. Zak and H. A. Shugart, Phys. Rev. A 6, 1715 (1972); see also R. H. Lambert and F. M. Pipkin, Phys. Rev. 129, 1233 (1963).

[3]K. M. Evenson and H. E. Radford, Phys. Rev. Lett. 15, 916 (1965).

[4]H. E. Radford and K. M. Evenson, Phys. Rev. 168, 70 (1968).

[5]J. W. McConkey, Phys. Lett. 12, 13 (1964).

[6]V. Kaufman and J. F. Ward, Appl. Opt. 6, 43 (1967).

[7]E. Clementi, C. C. J. Roothaan, and M. Yoshimine, Phys. Rev. 127, 1618 (1962).

[8]H. F. Schaefer III and R. A. Klemm, Phys. Rev. 188, 152 (1969).

[9]H. F. Schaefer III, R. A. Klemm, and F. E. Harris, Phys. Rev. 181, 137 (1969).

[10]H. F. Schaefer III, R. A. Klemm, and F. E. Harris, Phys. Rev. 176, 49 (1968).

[11]V. Beltrán-Lopez and T. Gonzalez E., Phys. Rev. A 2, 1651 (1970).

[12]G. J. Diebold, I. V. Rivas, S. Shafeizad, and D. L. McFadden, Chem. Phys. 52, 453 (1980).

[13]G. J. Diebold and D. L. McFadden, Rev. Sci. Instrum. 50, 157 (1979).

[14]E. U. Condon and G. H. Shortley, *The Theory of Atomic Spectra* (Cambridge University Press, London, 1935).

[15]S. Krongelb and M. W. P. Strandberg, J. Chem. Phys. 31, 1196 (1959).

[16]D. M. Brink and G. R. Satchler, *Angular Momentum* (Oxford University Press, London, 1968); B. Silver, *Irreducible Tensor Methods* (Academic, New York, 1976), p. 57.

[17]L. H. Aller, C. W. Ufford, and J. H. Van Vleck, Astrophys. J. 109, 43 (1949).

[18]A. Abragam and J. H. Van Vleck, Phys. Rev. 92, 1148 (1953).

[19]C. W. Ufford and R. M. Gilmour, Astrophys, J. 111, 580 (1950).

[20]J. S. M. Harvey, Proc. R. Soc. London A 285, 581 (1965).

[21]B. Bleany, in *Hyperfine Interactions,* edited by A. J. Freeman and R. B. Frenkel (Academic, New York, 1967).

[22]Note that the sign of ξ as given by the expressions in Refs. 20 or 21 is incorrect for the ^2D states of N. An alternate expressions for ξ can be obtained from Eqs. 3 and 26 in R. E. Trees, Phys. Rev. 92, 308 (1953); that is,

$$\begin{aligned}\xi=2\{&l(l+1)(2l+1)\\&\times[(2l-1)(2l+3)(2L-1)(2L+3)\\&\quad\times L(L+1)(2L+1)S(S+1)(2S+1)]^{-1}\}^{1/2}\\&\times(l^nSL\,||\vec{V}^{(12)}||\,l^nSL)\end{aligned}$$

for equivalent electrons, where the double barred matrix element is given in G. Racah, Phys. Rev. 63, 367 (1943). Expressions for the hyperfine coupling parameters can be verified through the sum rules given in S. Goudsmit, Phys. Rev. 37, 663 (1931).

[23]P. R. Bevington, *Data Reduction and Error Analysis for the Physical Sciences* (McGraw Hill, New York, 1969).

[24]There is some controversy over the ordering of the ^2P term. Theory (Ref. 19) predicts an inverted doublet, which contradicts the findings of a spectroscopic study (Ref. 6). Another experiment (Ref. 5) shows that complex excitation processes in a nitrogen plasma can give rise to line intensities that vary from point to point in the discharge. Table I was computed assuming an inverted term; however, if the EPR data are interpreted as arising from a normal doublet, we find that the values of the fine-structure interval and hyperfine coupling parameters are within the error limits given in Table I.

[25]C. Bauche-Arnoult, Proc. R. Soc. London A 322, 361 (1971).

[26]J. S. M. Harvey, L. Evans, and H. Lew, Can. J. Phys. 50, 1719 (1972).